Sciencexpress Research Article

Marine Radiocarbon Evidence for the Mechanism of Deglacial Atmospheric CO_2 Rise

T. M. Marchitto,[1,2]*† S. J. Lehman,[1,2]* J. D. Ortiz,[3] J. Flückiger,[2] A. van Geen[4]

[1]Department of Geological Sciences, University of Colorado, Boulder, CO 80309, USA. [2]Institute for Arctic and Alpine Research, University of Colorado, Boulder, CO 80309, USA. [3]Department of Geology, Kent State University, Kent, OH 44242, USA. [4]Lamont-Doherty Earth Observatory of Columbia University, Palisades, NY 10964, USA.

*These authors contributed equally to this work.

†To whom correspondence should be addressed. E-mail: tom.marchitto@colorado.edu

We reconstruct the radiocarbon activity of intermediate waters in the eastern North Pacific over the past 38,000 years. Radiocarbon activity paralleled that of the atmosphere except during deglaciation, when intermediate water values fell by more than 300‰. Such a large decrease requires a deglacial injection of very old waters from a deep ocean carbon reservoir that was previously well isolated from the atmosphere. The timing of intermediate water radiocarbon depletion closely matches that of atmospheric CO_2 rise, and effectively traces the redistribution of carbon from the deep ocean to the atmosphere during deglaciation.

Radiocarbon measurements of calendrically-dated hermatypic corals (*1*) and planktonic foraminifera (*2*, *3*) indicate that the radiocarbon activity ($\Delta^{14}C$) of the atmosphere varied between ~300‰ and 800‰ higher than today during the latter part of the last glacial period, ~20 to 40 kyr BP (Fig. 1C). Although reconstructions of Earth's geomagnetic field intensity predict higher cosmogenic ^{14}C production rates during this period, production was apparently not high enough to explain the atmospheric activities (*2*–*5*). Rather, a significant fraction of the atmosphere's $\Delta^{14}C$ buildup must have been due to decreased uptake of ^{14}C by the deep ocean. This requires a concomitant ^{14}C depletion in a deep ocean dissolved inorganic carbon reservoir that was relatively well isolated from the atmosphere. Renewed ventilation of this reservoir could theoretically explain the drop in atmospheric $\Delta^{14}C$ (Fig. 1C) and the rise in atmospheric CO_2 (*6*) across the last deglaciation. Most workers point to the Southern Ocean as a locus of deglacial CO_2 release, based on the similarity between atmospheric CO_2 and Antarctic temperature records (*6*) and on numerous conceptual and numerical models (e.g., *7*–*9*). If correct, we would expect some signature of the low-^{14}C deep carbon reservoir to be spread to other basins via Antarctic Intermediate Water (AAIW). Here we report a strong radiocarbon signal of the deglacial release of old carbon, recorded in an intermediate-depth sediment core from the northern edge of the eastern tropical North Pacific.

Multi-core/gravity-core/piston-core triplet MV99-MC19/GC31/PC08 was raised from 705 m water depth on the open margin off the western coast of southern Baja California (23.5°N, 111.6°W) (*10*). The site is today situated within the regional oxygen minimum zone that exists due to a combination of high export production and poor intermediate water ventilation. Various sediment properties in MC19/GC31/PC08 vary in concert with the so-called Dansgaard-Oeschger (D-O) cycles that characterized Northern Hemisphere climate during the last glacial period (*11*). Originally discovered in Greenland ice cores, D-O cycles also exist in a number of lower-latitude locations that were likely teleconnected to the North Atlantic region through the atmosphere (e.g., *2*, *12*, *13*). Off of Baja California, the sedimentary concentrations of organic carbon, Cd, Mo, and benthic foraminifera all decreased sharply during D-O stadials (cold periods in Greenland) (*11*, *14*). Together these proxies are consistent with reduced productivity during stadials, caused either by decreased coastal upwelling or by a deepening of the regional nutricline related to the mean state of the tropical Pacific (*11*).

Diffuse spectral reflectance (DSR) provides a 1-cm resolution stratigraphy for GC31/PC08. After R-mode factor analysis, the third factor of DSR (Fig. 1A) exhibits the strongest correlation to the productivity proxies and to Greenland climate (*11*). We use this DSR record to apply a calendar age model to MC19/GC31/PC08, based on correlation to $\delta^{18}O$ (an air temperature proxy) in Greenland ice core GISP2 (*15*). Resulting calendar ages are then combined with 50 benthic foraminiferal radiocarbon ages, 19 of which were published previously (*10*), to calculate age-corrected intermediate water $\Delta^{14}C$ (*16*). To evaluate the partitioning of ^{14}C between the atmosphere and ocean, we compare intermediate water $\Delta^{14}C$ to that of the atmosphere (Fig. 1C) as reconstructed from tree rings (*17*), U-Th-dated corals (*1*, *17*), and planktonic foraminifera from Cariaco Basin off of Venezuela (*3*). Calendar ages for Cariaco Basin were originally based on correlation of lithologic climate proxies to the GISP2 $\delta^{18}O$ record (*2*), which is layer counted using visual and chemical techniques (*15*). However, Hughen *et al.* (*3*) recently demonstrated that the Cariaco Basin ^{14}C calibration yields much better agreement with coral results older than ~22 kyr BP if an alternate age model is used, based on correlation to the U-Th-dated Hulu Cave speleothem $\delta^{18}O$ record from eastern China (*13*). Since DSR in GC31/PC08 is more similar to the Greenland isotope record than to the lower-resolution Hulu Cave record, we continue to use the GISP2 correlation but apply simple provisional age adjustments to GISP2 older than 23.4 kyr BP, using four tie-points to Hulu Cave (Fig. 1B, fig.S1). We do not suggest that this age model is necessarily superior to the original one (*15*), but this exercise is necessary for comparing our data to the most recent (and most consistent) atmospheric $\Delta^{14}C$ reconstructions (*1, 3, 17*). The resulting age model for MC19/GC31/PC08, based on 21 tie-points, yields a very constant sedimentation rate (fig. S2) and gives us confidence that our calendar age assignments for ^{14}C samples between tie-points are reliable to within a few hundred years (table S1).

Baja California intermediate water radiocarbon activities are plotted in red in Fig. 1C. The modern activity, based on a local seawater measurement of –131‰ at 445 m and the nearest GEOSECS profile (*18*), is estimated to be –170‰, in good agreement with the core top value. Comparable offsets from the contemporaneous atmosphere were maintained throughout the Holocene (typically ~100‰ between 0-10 kyr BP) and during the latter part of the glacial period (roughly 200‰ between 20-30 kyr BP) (*19*). Radiocarbon activities prior to 30 kyr BP show increased scatter which may be related to the fact that slight contaminations have greater influence on older samples.

Overall it is clear that intermediate waters mainly followed atmospheric $\Delta^{14}C$ over the past 40 kyr, except during the last deglaciation. Activities dropped sharply just after 18 kyr BP, reaching minimum values of ~–180‰ between 15.7 and 14.6 kyr BP, roughly 450‰ lower than the contemporaneous atmosphere. For comparison, the lowest $\Delta^{14}C$ values found in the modern ocean (in the North Pacific near 2 km water depth) are depleted by ~240‰ relative to the pre-industrial atmosphere (*18*). A second comparably large depletion event began sometime between 13.5 and 12.9 kyr BP and ended between 12.1 and 11.6 kyr BP. The magnitude of ^{14}C depletion we reconstruct during these two deglacial events is much too great to attribute to changes in dynamics of the North Pacific thermocline (*20*), and must instead record a large change in the initial ^{14}C activity of waters advected to the site. Such depleted waters could have been sourced only from the deepest, most isolated regions of the glacial ocean (*21*).

In Fig. 2 we compare the timing of reconstructed intermediate water and atmospheric $\Delta^{14}C$ changes with the deglacial record of atmospheric CO_2 from the East Antarctic Dome C ice core (*6*). The latter is shown on a GISP2 layer-counted timescale based on a simple synchronization of methane variations between the Dome C and GISP2 ice cores (supporting online text, table S2). It is immediately apparent that the atmospheric $\Delta^{14}C$ decline and CO_2 rise occurred in parallel, with a synchronous, intervening plateau appearing in both records. There is a slight (and still unreconciled) difference in timing of the start of the deglacial atmospheric $\Delta^{14}C$ decline between the Cariaco Basin (*3*) and IntCal04 (*17*) reconstructions, but we take the deglacial onset of the atmospheric CO_2 rise and the atmospheric ^{14}C decline to be essentially synchronous. We now also find that these changes were associated with a prominent decline in $\Delta^{14}C$ of intermediate water in the eastern North Pacific that must record the redistribution of aged carbon from the deep ocean to the surface. After 14.6 kyr BP intermediate water activities rebounded to higher values, coincident with the plateau in both the atmospheric CO_2 rise and the atmospheric $\Delta^{14}C$ drop. The leveling of the atmospheric records and the increase in ^{14}C activity of intermediate waters are all indicative of a reduction in the flux of aged carbon to the upper ocean and atmosphere from below. After ~12.8 kyr BP the atmospheric CO_2 rise and $\Delta^{14}C$ drop resumed, and intermediate water activities again reached minimum values of ~–180‰, indicating a resumption of carbon redistribution from the deep ocean to the surface. By 11.5 kyr BP the large deglacial atmospheric shifts were largely completed and intermediate water activities finally reached modern values.

As pointed out by Monnin *et al.* (*6*), the deglacial rise of atmospheric CO_2 closely followed the rise in East Antarctic temperatures (Fig. 3A), implying that the ocean's release of carbon to the atmosphere was associated with changes in the Southern Ocean. Deep convection of the Southern Ocean both ventilates much of the ocean interior and returns to the atmosphere much of the carbon extracted by photosynthesis in the sunlit surface of the global ocean. During the last glacial period, density stratification of the Southern Ocean surface and/or extensive sea ice coverage are suggested to have isolated deep waters from the atmosphere (e.g., *7–9*), permitting the buildup of a larger deep ocean carbon reservoir and a consequent drawdown of atmospheric CO_2. Sediment pore water chlorinity and $\delta^{18}O$ measurements, combined with benthic foraminiferal $\delta^{18}O$, indicate that deep Southern Ocean waters were the saltiest and densest waters in the glacial ocean (*22*). Such high salinities point to brine formation beneath sea ice as an important mode of formation. At deglaciation, a progressive renewal of deep convection or upwelling in association with documented sea-ice retreat (*23*) [and possibly with poleward-shifting westerlies (*8*)] would have provided for the simultaneous delivery of ocean heat and sequestered carbon to the atmosphere. This transition occurred in two major steps, beginning with relatively early (~18 kyr) and gradual increases in temperature and CO_2 that were temporarily interrupted by the Antarctic Cold Reversal (ACR). Major transients in our record of $\Delta^{14}C$ in intermediate depth waters of the eastern North Pacific conform to this Antarctic schedule, consistent with the redistribution of carbon from the abyss to the upper ocean and atmosphere in connection with changes in deep convection of the Southern Ocean.

$\delta^{13}C$ provides a tracer that is complementary to $\Delta^{14}C$, though with a far smaller dynamic range in seawater. During the last glacial period, the deep Southern Ocean contained the ocean's lowest $\delta^{13}C$ values, suggesting a local accumulation of remineralized carbon and/or poor ventilation (*24*). Spero and Lea (*25*) argued that during the early part of the last deglaciation, Southern Ocean sea ice retreat (*23*) combined with increased deep convection and northward Ekman transport imparted transient low $\delta^{13}C$ values to AAIW and Subantarctic Mode Waters (SAMW), and that this signal was recorded by deep dwelling planktonic foraminifera in various ocean basins, including the eastern tropical North Pacific. These waters should also have carried a low $\Delta^{14}C$ signature, and we suggest that this is the signal we observe off of Baja California. Today AAIW is barely traceable as a distinct water mass north of the equator in the eastern tropical Pacific (*26*). We argue that the northward penetration of AAIW during deglaciation was greater than today (*27*) and was at times fed by extremely ^{14}C-depleted waters sourced from the abyss by deep overturning in the Southern Ocean. Sea ice retreat could have allowed upwelled deep waters to gain buoyancy from precipitation, converting some fraction of these waters into AAIW without substantial mixing with warmer thermocline waters (*28*), which would otherwise dampen the $\Delta^{14}C$ signal. There is evidence that vertical stratification of the North Pacific also varied on an Antarctic climate schedule (*29*), so northern deep waters may have supplemented the supply of aged carbon to the Baja California site. However, the interaction of strong circum-polar winds with bathymetry in the Southern Ocean provides for much more effective vertical pumping (*30*) than do conditions in the North Pacific, and therefore southern sources most likely dominated the $\Delta^{14}C$ changes in our record.

Numerous observational and modeling studies indicate an inverse relationship between Antarctic and North Atlantic temperature variations that may be due to altered inter-hemispheric ocean heat transport and/or opposing local deep water formation histories (e.g., *28*, *31–33*). Insofar as $\Delta^{14}C$ of the intermediate-depth Pacific provides an inverse proxy for the strength of deep convection in the Southern Ocean, our results are strong evidence for tight, inverse coupling of deep water formation between hemispheres. This is clearly demonstrated by the co-variation of intermediate-depth Pacific $\Delta^{14}C$ and the formation history of North Atlantic Deep Water (NADW) [or its glacial analog, Glacial North Atlantic Intermediate Water (GNAIW)] based on measurements of $^{231}Pa/^{230}Th$ from sediments in the western North Atlantic (*34*) (Fig. 3C). The near-cessation of ^{231}Pa export beginning just after 18 kyr BP records a collapse of GNAIW that has been linked to a massive discharge of glacial ice and fresh water to the North Atlantic known as Heinrich event 1. Following a recovery during the Bølling-Allerød warm phase, another marked weakening of NADW/GNAIW is documented during the Younger Dryas cold period, most likely also triggered by a discharge of glacial meltwater (*34*). Both periods of NADW/GNAIW reduction were times of intermediate-depth Pacific $\Delta^{14}C$ decline and atmospheric CO_2 rise.

It is often difficult to identify triggers in a tightly coupled system, but the relationships described above suggest that the Antarctic climate schedule may have been paced by ice sheet and meltwater forcing around the North Atlantic. Support for this comes from our observation that while major inflections in the $\Delta^{14}C$ and $^{231}Pa/^{230}Th$ records in Fig. 3 are almost exactly synchronous, the large $\Delta^{14}C$ decrease (i.e., Southern Ocean ventilation increase) during Heinrich event 1 occurred more gradually than the associated decrease in GNAIW export. This relationship is consistent with the relatively slow response of southern warming via hypothesized anomalous heat transport (e.g, *33*), with associated sea ice retreat (*23*) [and possibly poleward-shifting westerlies (*8*)] leading to progressive increases in deep overturning and ventilation of the Southern Ocean. Alternatively, Southern Ocean overturning may have been instigated by NADW/GNAIW reductions through the requirement (*35*) that global rates of deep water formation balance global deep upwelling, which is forced mainly by winds and tides. The abrupt rise in atmospheric $\Delta^{14}C$ at the start of the Younger Dryas [+80‰ in just 180 yr (*36*)] (Fig. 2) may record the time elapsed before the Southern Ocean could begin responding to reduced NADW formation, leading to the brief absence of deep ocean sinks for ^{14}C (*32*).

Recent work shows that deep North Atlantic radiocarbon activities increased abruptly during the Bølling-Allerød due to renewed formation of NADW, and temporarily decreased again during the Younger Dryas (*37*). In light of our new record, this is clearly a North Atlantic pattern (arising from deep circulation changes within the basin), while the anti-phased intermediate-depth North Pacific record tracks the overall redistribution of carbon from the deep ocean to the atmosphere.

Finally, our results bear on recent questions concerning reconstructed rates of atmospheric $\Delta^{14}C$ decline during deglaciation and implied ^{14}C aging of glacial deep waters. Although subject to uncertainties (*19*), decay projection of our first deglacial $\Delta^{14}C$ minimum back to the surface ocean (*38*) gives an apparent ventilation age of ~4000 yr, implying that the inferred deep Southern Ocean source waters were at least that old. This is broadly consistent with the minimum deep ocean age estimated from the atmospheric record, assuming the old reservoir filled half of the ocean's volume (*39*). Ages as great as 5000 yr have been reported for glacial deep waters near New Zealand (*40*), but more northerly sites in the Pacific show little difference from today, at least shallower than ~2 km (*39*). We infer that the greatest ^{14}C depletion of the glacial deep ocean was most likely concentrated in the Southern Ocean region (and deepest Pacific), coincident with highest densities (*22*) and lowest $\delta^{13}C$ values (*24*).

References and Notes

1. R. G. Fairbanks *et al.*, *Quaternary Science Reviews* **24**, 1781 (2005).
2. K. Hughen *et al.*, *Science* **303**, 202 (2004).
3. K. Hughen, J. Southon, S. J. Lehman, C. Bertrand, J. Turnbull, *Quaternary Science Reviews* **25**, 3216 (2006).
4. C. Laj *et al.*, *Earth and Planetary Science Letters* **200**, 177 (2002).
5. R. Muscheler *et al.*, *Earth and Planetary Science Letters* **219**, 325 (2004).
6. E. Monnin *et al.*, *Science* **291**, 112 (2001).
7. D. M. Sigman, E. A. Boyle, *Nature* **407**, 859 (2000).
8. J. R. Toggweiler, J. L. Russell, S. R. Carson, *Paleoceanography* **21**, doi:10.1029/2005PA001154 (2006).
9. B. B. Stephens, R. F. Keeling, *Nature* **404**, 171 (2000).
10. A. van Geen *et al.*, *Paleoceanography* **18**, doi:10.1029/2003PA000911 (2003).
11. J. D. Ortiz *et al.*, *Geology* **32**, 521 (2004).
12. R. J. Behl, J. P. Kennett, *Nature* **379**, 243 (1996).
13. Y. J. Wang *et al.*, *Science* **294**, 2345 (2001).
14. W. E. Dean, Y. Zheng, J. D. Ortiz, A. van Geen, *Paleoceanography* **21**, doi:10.1029/2005PA001239 (2006).
15. P. M. Grootes, M. Stuiver, *Journal of Geophysical Research* **102**, 26455 (1997).
16. Methods are available as supporting material on *Science* Online. In the supporting material we also present our $\Delta^{14}C$ calculated using the original GISP2 chronology (*15*), and compare it to the original Cariaco record based on correlation to GISP2 (*2*) (fig. S3).
17. P. J. Reimer, et al., *Radiocarbon* **46**, 1029 (2004).
18. G. Ostlund, H. Craig, W. S. Broecker, D. Spencer, *GEOSECS Atlantic, Pacific and Indian Ocean Expeditions, Vol. 7, Shorebased Data and Graphics* (U.S. Government Printing Office, Washington, DC, 1987).
19. Throughout most of this paper we discuss our $\Delta^{14}C$ values with respect to the contemporaneous atmosphere rather than calculating ventilation ages by decay projection (*38*) because of large uncertainties in initial surface ocean reservoir ages and the possibility of multiple intermediate/deep water sources with different ventilation histories.
20. U. Mikolajewicz, T. J. Crowley, A. Schiller, R. Voss, *Nature* **387**, 384 (1997).
21. The deglacial injection of low-^{14}C intermediate waters along the Baja California margin did not noticeably overprint the DSR or other O_2-sensitive productivity proxies recorded in GC31/PC08. Although $\Delta^{14}C$ and O_2 are broadly correlated in the modern ocean, they can also be decoupled (*18*), for example through air-sea exchange. Hence deglacial intermediate waters were very depleted in $\Delta^{14}C$ but apparently not drastically depleted in O_2.
22. J. F. Adkins, K. McIntyre, D. P. Schrag, *Science* **298**, 1769 (2002).
23. R. Gersonde, X. Crosta, A. Abelmann, L. Armand, *Quaternary Science Reviews* **24**, 869 (2005).
24. U. S. Ninnemann, C. D. Charles, *Earth and Planetary Science Letters* **201**, 383 (2002).
25. H. J. Spero, D. W. Lea, *Science* **296**, 522 (2002).
26. P. C. Fiedler, L. D. Talley, *Progress in Oceanography* **69**, 143 (2006).
27. S. Schulte, F. Rostek, E. Bard, J. Rullkötter, O. Marchal, *Earth and Planetary Science Letters* **173**, 205 (1999).
28. R. F. Keeling, B. B. Stephens, *Paleoceanography* **16**, 112 (2001).
29. S. L. Jaccard *et al.*, *Science* **308**, 1003 (2005).
30. J. R. Toggweiler, B. Samuels, *Deep-Sea Research I* **42**, 477 (1995).
31. T. J. Crowley, *Paleoceanography* **7**, 489 (1992).
32. W. S. Broecker, *Paleoceanography* **13**, 119 (1998).
33. R. Knutti, J. Flückiger, T. F. Stocker, A. Timmermann, *Nature* **430**, 851 (2004).
34. J. F. McManus, R. Francois, J.-M. Gherardi, L. D. Keigwin, S. Brown-Leger, *Nature* **428**, 834 (2004).
35. W. Munk, C. Wunsch, *Deep-Sea Research I* **45**, 1977 (1998).
36. K. A. Hughen, J. R. Southon, S. J. Lehman, J. T. Overpeck, *Science* **290**, 1951 (2000).
37. L. F. Robinson *et al.*, *Science* **310**, 1469 (2005).
38. J. F. Adkins, E. A. Boyle, *Paleoceanography* **12**, 337 (1997).
39. W. S. Broecker *et al.*, *Science* **306**, 1169 (2004).
40. E. L. Sikes, C. R. Samson, T. P. Guilderson, W. R. Howard, *Nature* **405**, 555 (2000).

41. We thank D. Lopez, J. Turnbull, and C. Wolak for laboratory assistance; J. Southon for AMS analyses; A. Pearson for providing an unpublished seawater $\Delta^{14}C$ measurement; and T. Blunier for providing Dome C EDC3 time scale and for valuable discussions on synchronization

of the different ice cores. This manuscript was improved by comments from R. Keeling and two anonymous reviewers. Support was provided by NSF grants OCE-9809026 and OCE-0214221.

Supporting Online Material
www.sciencemag.org/cgi/content/full/1138679/DC1
Materials and Methods
SOM Text
Figs. S1 to S3
Tables S1 and S2
References

11 December 2006; accepted 27 April 2007
Published online 10 May 2007; 10.1126/science.1138679
Include this information when citing this paper.

Fig. 1. Intermediate water and atmospheric $\Delta^{14}C$ records. (**A**) Diffuse spectral reflectance factor 3 from Baja California composite sediment core MV99-GC31/PC08, plotted versus depth (top axis) (*11*). Gray lines show tie-points to Greenland record used to derive calendar age model. (**B**) $\delta^{18}O$ of Greenland ice core GISP2 (*15*) on provisional revised timescale (black, bottom axis). New timescale deviates from original timescale (green) older than 23.4 kyr BP (line labeled G). New timescale is based on linear interpolation between point G and three tie-points whose ages are derived from U-Th-dated Hulu Cave (lines labeled H) (*13*). (**C**) Atmospheric radiocarbon activities based on tree rings, planktonic foraminifera from Cariaco Basin varve-counted sediments, and U-Th-dated corals (dark green) (*17*); additional recent coral measurements (cyan) (*1*); and planktonic foraminifera from Cariaco Basin using age model derived from reflectance correlation to Hulu Cave (blue) (*3*). Red points show intermediate water activities from benthic foraminifera in MC19/GC31/PC08. Yellow point is estimate for modern bottom waters at this site.

Fig. 2. Baja California intermediate water $\Delta^{14}C$ during the last deglaciation (red) compared to atmospheric $\Delta^{14}C$ (dark green, cyan, and blue) (*1*, *3*, *17*) and atmospheric CO_2 from Antarctica Dome C (*6*) placed on GISP2 timescale (black). Dashed gray lines show ages of Bølling-Allerød (B–A) and Younger Dryas (YD) boundaries based on GISP2 $\delta^{18}O$ record, and start of Heinrich event 1 (H1) based on $^{231}Pa/^{230}Th$ record from Bermuda Rise (*34*). The Antarctic Cold Reversal (ACR) is contemporaneous with the Bølling-Allerød.

Fig. 3. Southern and northern ocean-atmosphere changes during the last deglaciation, compared to intermediate water $\Delta^{14}C$. (**A**) Atmospheric CO_2 (black) and ice δD temperature proxy (cyan) from Antarctica Dome C (*6*) placed on GISP2 timescale. (**B**) Baja California intermediate water $\Delta^{14}C$. (**C**) Inverted decay-corrected excess $^{231}Pa/^{230}Th$ in Bermuda Rise sediments, using two methods to calculate excess (dark green and purple) (*34*). Horizontal dashed line shows water column production ratio for these isotopes (0.093); lower values are primarily due to Pa export by vigorous NADW. Vertical dashed lines show ages of climatic boundaries as in Fig. 2.

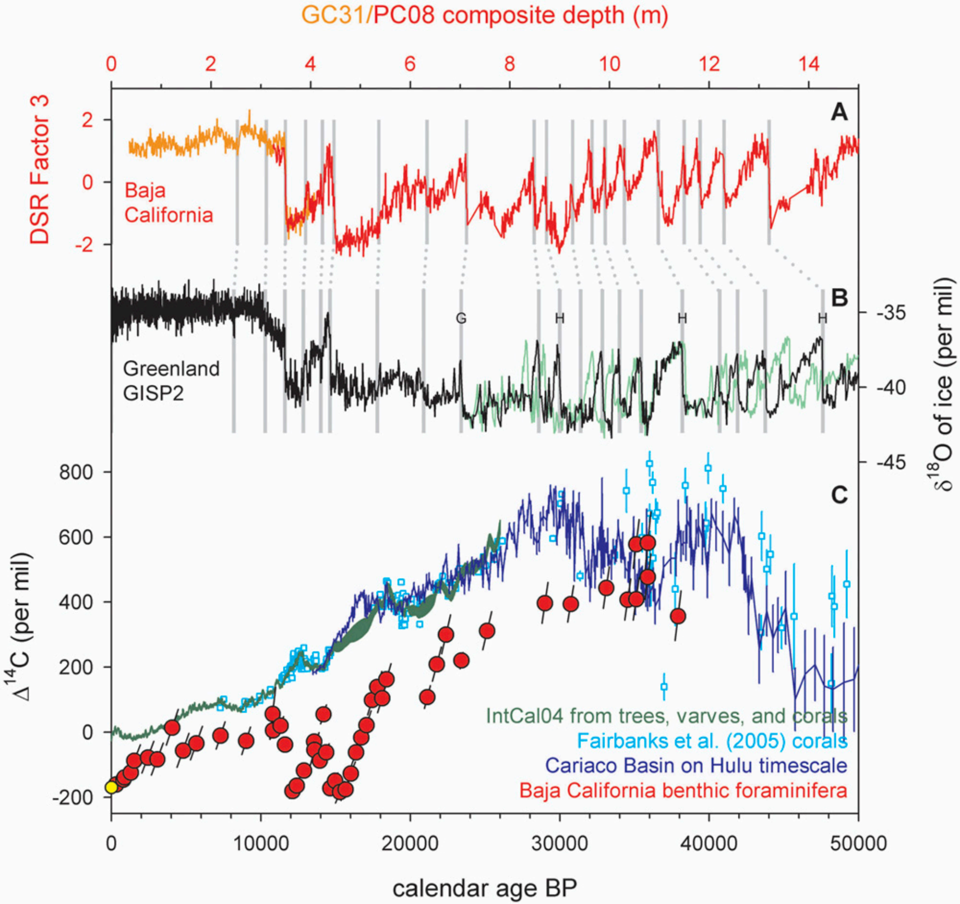

GC31/PC08 composite depth (m)
DSR Factor 3
A
Baja California
B
G
H
H
H
Greenland GISP2
δ18O of ice (per mil)
C
Δ14C (per mil)
IntCal04 from trees, varves, and corals
Fairbanks et al. (2005) corals
Cariaco Basin on Hulu timescale
Baja California benthic foraminifera
calendar age BP

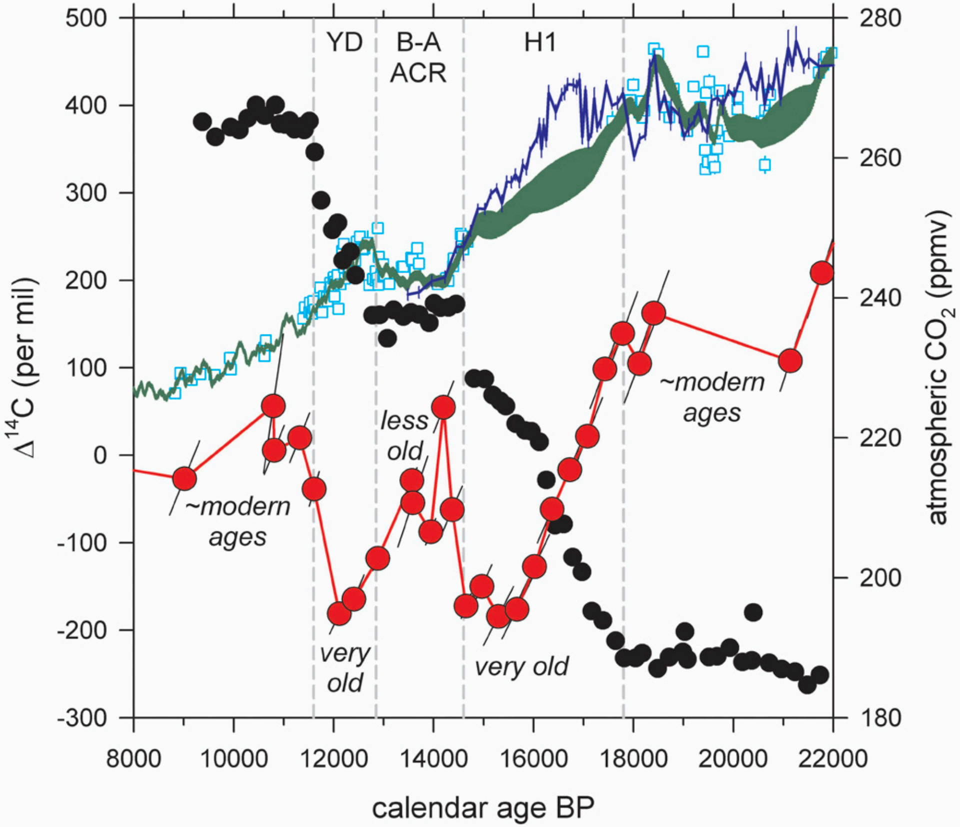

YD
B-A
ACR
H1
~modern ages
less old
very old
very old
~modern ages
Δ14C (per mil)
atmospheric CO2 (ppmv)
calendar age BP
500
400
300
200
100
0
-100
-200
-300
280
260
240
220
200
180
8000
10000
12000
14000
16000
18000
20000
22000

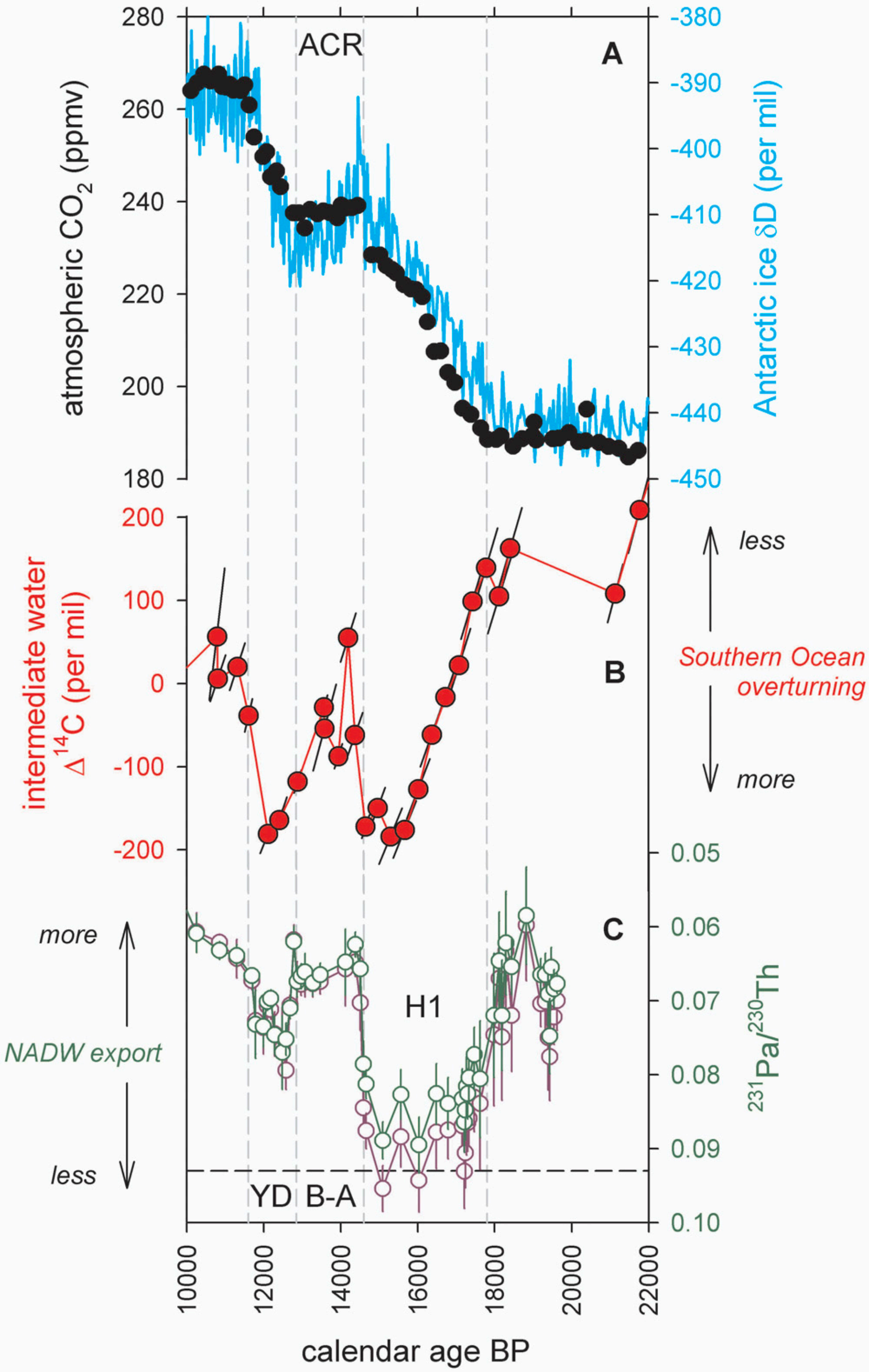

ACR
A
B
C
atmospheric CO_2 (ppmv)
Antarctic ice δD (per mil)
intermediate water $\Delta^{14}C$ (per mil)
less
Southern Ocean overturning
more
more
NADW export
less
H1
YD
B-A
$^{231}Pa/^{230}Th$
calendar age BP
280
260
240
220
200
180
-380
-390
-400
-410
-420
-430
-440
-450
200
100
0
-100
-200
0.05
0.06
0.07
0.08
0.09
0.10
10000
12000
14000
16000
18000
20000
22000